

Nematic Bogoliubov Fermi surfaces from magnetic toroidal order in $\text{FeSe}_{1-x}\text{S}_x$

Hao Wu,^{1,*} Adil Amin,^{1,*} Yue Yu,¹ and Daniel F. Agterberg¹

¹*Department of Physics, University of Wisconsin–Milwaukee, Milwaukee, Wisconsin 53201, USA*

(Dated: June 29, 2023)

Recently it has been argued that the superconducting state of $\text{FeSe}_{1-x}\text{S}_x$ exhibits Bogoliubov Fermi surfaces for $x > 0.17$. These Bogoliubov Fermi surfaces appear together with broken time-reversal symmetry and surprisingly demonstrate nematic behavior in a structurally tetragonal phase. Through a symmetry-based analysis of Bogoliubov Fermi surfaces that can arise from broken time-reversal symmetry, we argue that the likely origin of time-reversal symmetry breaking is due to magnetic toroidal order. We show that this magnetic toroidal order naturally appears as a consequence of either static Néel antiferromagnetic order or due to the formation of a spontaneous pair density wave superconducting order. Finally, we reveal that independent of the presence of Bogoliubov Fermi surfaces, supercurrents will induce Néel magnetic order in many Fe-based superconductors.

Introduction.—Among the iron-based superconductors [1], iron selenide (FeSe), with the simplest crystal structure and chemical composition, has attracted much attention [2–5]. It adopts a tetragonal structure at room temperature. Upon cooling, there is a structural transition from tetragonal to orthorhombic (nematic) at low temperature under ambient pressure [6–8]. However, the nematicity in the isovalently substituted $\text{FeSe}_{1-x}\text{S}_x$ [9, 10] is strongly suppressed with sulfur (S) doping [11, 12], and it is completely suppressed at a sulfur content $x \approx 0.17$, indicating a nematic quantum critical point [13].

In the tetragonal phase of $\text{FeSe}_{1-x}\text{S}_x$, there are experimental signatures for Fermi surfaces in the superconducting state. In particular, these Bogoliubov Fermi surfaces (BFSs) [14, 15] reveal themselves through a large residual density of states (DOS) at the chemical potential has been observed in the superconducting state through specific heat, thermal conductivity, and scanning tunneling spectroscopy (STS) measurements [16–18]. Furthermore, evidence for broken time-reversal symmetry in $\text{FeSe}_{1-x}\text{S}_x$ by muon spin relaxation (μSR) measurements has also appeared [19]. Time-reversal symmetry breaking (TRSB) is known to play a central role in stabilizing BFSs [14, 20–29]. TRSB, together with the preservation of parity symmetry, has been argued to give rise to topologically protected BFSs in $\text{FeSe}_{1-x}\text{S}_x$ [19, 28, 29], however, the detailed microscopic mechanism for these BFSs remains unclear.

More recently, laser-based angle-resolved photoemission spectroscopy (laser ARPES) has directly observed a BFS in the tetragonal phase of $\text{FeSe}_{1-x}\text{S}_x$ [30]. Surprisingly, this BFS has nematic symmetry, even though $\text{FeSe}_{1-x}\text{S}_x$ is structurally tetragonal. Here, we use a symmetry-based analysis of BFSs to argue that the most likely origin of such a nematic BFS is a magnetic toroidal (MT) order [31–42]. This order differs from previous suggestions [19, 28, 29] of a parity-preserving TRSB order in that the magnetic toroidal order breaks both parity symmetry (\mathcal{P}) and time-reversal symmetry (\mathcal{T}) while pre-

servicing the product of the two. We find that both the shape of the BFS and the momentum dependence of the minimum of the quasi-particle excitation energy are consistent with the laser ARPES results [30].

We suggest two different possible origins for the magnetic toroidal order: the appearance of static Néel antiferromagnetic (AFM) order with moments aligned in-plane, or the formation of a spontaneous pair density wave (PDW) superconducting order with an order parameter $\psi = \psi_0 e^{i\mathbf{q}\cdot\mathbf{r}}$. For the AFM order to give rise to the BFSs in the superconducting state, it must order at a temperature higher than the superconducting T_c . For the spontaneous PDW state formation, the BFSs appear with PDW order at the superconducting T_c independently of any AFM order. Like magnetic toroidal order, both the AFM order and PDW order are \mathcal{P} -breaking, \mathcal{T} -breaking, and \mathcal{PT} -preserving. Furthermore, the momentum \mathbf{q} of the PDW order [43] and the AFM order both belong to the same E_u irreducible representation (irrep) of the D_{4h} point group. This implies that in the superconducting state, these two orders are coupled. Consequently, superconductivity forming in the presence of an already ordered AFM state will be a PDW state by symmetry (see the companion paper [44]). In addition, if a spontaneous PDW order appears at T_c , symmetry requires that AFM order will also appear at the superconducting T_c . More generally, this coupling implies that an in-plane supercurrent in any $P4/nmm$ Fe-based superconductors will generically induce AFM order with the moment in-plane.

Symmetry analysis of BFSs.—All existing mechanisms for the appearance of BFSs require a translation invariant TRSB order [14, 20–22, 29]. Here we carry out a symmetry analysis of the role of this TRSB on the Bogoliubov quasi-particle spectrum. We explicitly consider the single-band limit in this analysis. While Fe-based superconductors are multiband systems [5], the observed low T_c in $\text{FeSe}_{1-x}\text{S}_x$ suggests that interband pairing interactions will not significantly alter the Bogoliubov quasi-particle spectrum, so a single-band analysis should suf-

fice.

In our analysis, the key interaction is due to the TRSB, which alters the normal state Hamiltonian. This interaction can be external or induced by the broken time-reversal symmetry in the superconducting state [14, 45], the origin of this term is not essential for our analysis of the quasi-particle spectrum. For a single-band, with two pseudospin degrees of freedom, the normal state Hamiltonian with TRSB takes the general form

$$H_N = [\xi_+(\mathbf{k}) + \xi_-(\mathbf{k})]\sigma_0 + \mathbf{h}(\mathbf{k}) \cdot \vec{\sigma} \quad (1)$$

here the Pauli matrices σ_i describe the spin degrees of freedom, $\xi_+(-\mathbf{k}) = \xi_+(\mathbf{k})$, $\xi_-(-\mathbf{k}) = -\xi_-(\mathbf{k})$, and $\mathbf{h}(-\mathbf{k}) = \mathbf{h}(\mathbf{k})$. The interaction $\xi_-(\mathbf{k})$ describes parity-odd time-reversal symmetry breaking while $\mathbf{h}(\mathbf{k})$ describes parity-even time-reversal symmetry breaking. These interactions can further be classified by which irrep of the D_{4h} point group they belong to. Furthermore, since the observed BFSs are near the Γ point, we carry out a power series expansion in momentum for $\xi_-(\mathbf{k})$ and $\mathbf{h}(\mathbf{k})$ consistent with the symmetry properties defined by the corresponding irrep. These interactions, together with the resulting BFSs are given in Table I. For simplicity, we take $\xi_+(\mathbf{k}) = \frac{\hbar^2(k_x^2 + k_y^2)}{2m}$. For $\text{FeSe}_{1-x}\text{S}_x$, the normal state dispersion near the Γ -point has a weak k_z dependence and also has a four-fold in-plane anisotropy, but this will not qualitatively change the results.

To describe the superconducting state we assume singlet pairing with an anisotropic s -wave gap given by $\psi(\mathbf{k}) = \Delta_0 + \Delta_4 \cos(4\theta)$ with $\Delta_0 > 0$, $\Delta_4 < 0$, and $\Delta_0 > |\Delta_4|$, where θ is the polar angle for the in-plane momentum \mathbf{k} [4].

The Bogoliubov quasi-particle spectrum depends upon the parity of the TRSB [14, 15]. For even \mathcal{P} , it takes the form [14, 15]

$$E_{\mathbf{k},\pm,\nu} = \nu |\mathbf{h}(\mathbf{k})| \pm \sqrt{[\xi_+(\mathbf{k}) - \mu]^2 + |\psi(\mathbf{k})|^2}, \quad (2)$$

where $\nu = \pm 1$ and μ is the chemical potential. For odd \mathcal{P} , this dispersion has been discussed in the companion paper [44] and takes the form

$$E_{\mathbf{k},\pm} = \xi_-(\mathbf{k}) \pm \sqrt{[\xi_+(\mathbf{k}) - \mu]^2 + |\psi(\mathbf{k})|^2}. \quad (3)$$

For Eq. (2), BFSs occur for \mathbf{k} when $|\mathbf{h}(\mathbf{k})| > |\psi(\mathbf{k})|$ while for Eq. (3) they occur for $|\xi_-(\mathbf{k})| > |\psi(\mathbf{k})|$. In Table I, we show the possible BFSs that arise from Eqs. (2) and (3). Note we choose values of the parameters such that the spectrum contains BFSs. We have further chosen a finite value of k_z when terms in either $\xi_-(\mathbf{k})$ and $\mathbf{h}(\mathbf{k})$ vanish by symmetry when $k_z = 0$. Importantly, the only irreps which allow the appearance of a nematic BFS are the E_g and E_u irreps. For all the other irreps, the tetragonal symmetry is not broken. For the E_g irrep, however, the nematic BFS appears only when k_z is finite, when $k_z = 0$ a tetragonal BFS appears. Note that in Ref. [28],

Irrep	$\mathbf{h}(\mathbf{k})$	BFS	Irrep	$\xi_-(\mathbf{k})$	BFS
A_{1g}	$h_1(k_y k_z \hat{x} - k_x k_z \hat{y}) + h_2 k_x k_y (k_x^2 - k_y^2) \hat{z}$		A_{1u}	$\alpha k_x k_y k_z \times (k_x^2 - k_y^2)$	
A_{2g}	$h_1(k_x k_z \hat{x} + k_y k_z \hat{y}) + h_2 \hat{z}$		A_{2u}	αk_z	
B_{1g}	$h_1(k_y k_z \hat{x} + k_x k_z \hat{y}) + h_2 k_x k_y \hat{z}$		B_{1u}	$\alpha k_x k_y k_z$	
B_{2g}	$h_1(k_x k_z \hat{x} - k_y k_z \hat{y}) + h_2(k_x^2 - k_y^2) \hat{z}$		B_{2u}	$\alpha k_z (k_x^2 - k_y^2)$	
E_g	$h_{1x} \hat{x} + h_{1y} \hat{y} + (h_{2x} k_x k_z + h_{2y} k_y k_z) \hat{z}$		E_u	$T_x k_x + T_y k_y$	

TABLE I. Structures of $\mathbf{h}(\mathbf{k})$ and $\xi_-(\mathbf{k})$ for \mathcal{T} -breaking order belonging to D_{4h} point group irreps and the corresponding BFSs. We express momenta k in units of the Fermi momentum $k_F = \frac{\sqrt{2m\mu}}{\hbar}$ and energies in units of the maximum gap $\Delta_{max} = \Delta_0 + |\Delta_4|$. In units Δ_{max} , we take $\mu = 2.2361$, $\Delta_0 = 0.6545$, $\Delta_4 = -0.3455$. The other parameters in units Δ_{max} are chosen as: for A_{1g} , $h_1 k_z k_F = 0.6325$, $h_2 k_F^4 = 0.7071$; for A_{2g} , $h_1 k_z k_F = 0.3162$, $h_2 = 0.8944$; for B_{1g} , $h_1 k_z k_F = 0.7746$, $h_2 k_F^2 = 0.8944$; for B_{2g} , $h_1 k_z k_F = 0.7746$, $h_2 k_F^2 = 0.8944$; for E_g , $h_{1x} = 0.3$, $h_{1y} = 0$, $h_{2x} k_z k_F = 0.8944$, $h_{2y} k_z k_F = 0$; for A_{1u} , $\alpha k_z k_F^4 = 2.3$; for A_{2u} , $\alpha k_z = 0.95$; for B_{1u} , $\alpha k_z k_F^2 = 2.2$; for B_{2u} , $\alpha k_z k_F^2 = 1$; for E_u , $T_x k_F = 0.95$ and $T_y k_F = 0$.

the parity-preserving, broken time-reversal symmetry belongs to E_g irrep. While an E_g irrep leads to nematic BFSs in principle, we note that the TRSB consistent with this E_g irrep implies the existence of ferromagnetic order with the moment in the plane. Such order has not been observed in the $\text{FeSe}_{1-x}\text{S}_x$ [19], so we expect the more likely candidate is the E_u irrep.

For TRSB belonging to the E_u irrep, we can further compare the predicted minimum of the quasi-particle excitation energy with the experimentally observed value. The computed minimum energy gap function of the polar angle is shown in Fig. 1. This agrees well with laser ARPES measurements [30].

Origin of magnetic toroidal order.—The above symmetry-based analysis suggests that the TRSB that gives rise to the observed BFSs is a magnetic toroidal order belonging to an E_u irrep. Here we show that there are two possible microscopic origins for this order: Néel AFM order with the moment oriented in plane or the spontaneous formation of a PDW phase. We initially discuss the Néel AFM order.

In Fig. 2 we show the Néel AFM order that belongs to the E_u irrep. Key to understanding how this Néel ordered state is odd under parity symmetry is the non-symmorphic $P4/nmm$ space group of tetragonal $\text{FeSe}_{1-x}\text{S}_x$. This space group requires that there are two Fe atoms per unit cell related by an inversion center. Consequently, when the moments on these two Fe sites are oriented in opposite directions, the magnetic state is

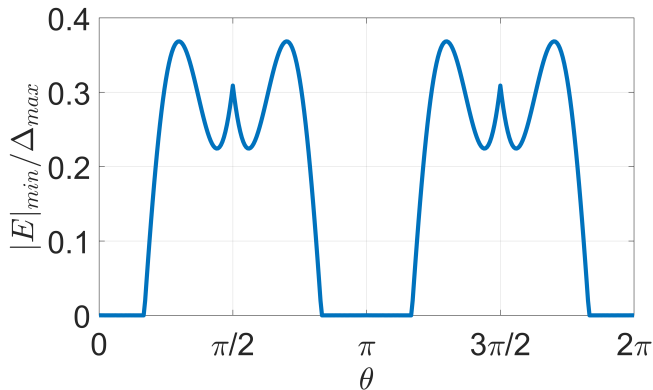


FIG. 1. Minimum single-particle energy gap as a function of polar angle predicted for $\text{FeSe}_{1-x}\text{S}_x$ near the Γ point. For each angle θ , the minimum energy gap occurs for a momentum approximately equal to k_F , the Fermi momentum. The extended region of a zero energy gap is the predicted Bogoliubov Fermi surface.

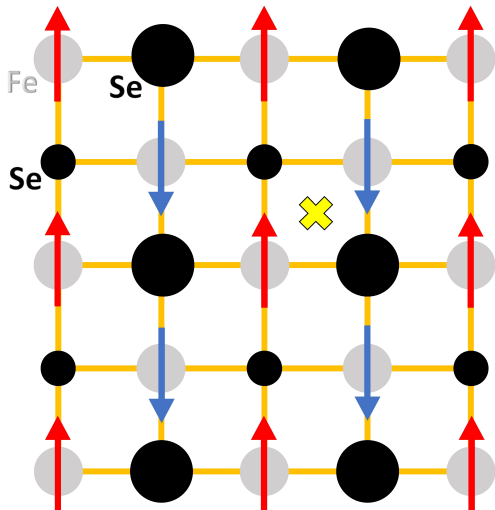


FIG. 2. Néel antiferromagnetic order that serves as a magnetic toroidal order. The selenium atoms with bigger (smaller) sizes reside above (below) the iron layer. The yellow cross is the lattice inversion center. The red and blue arrows indicate the direction of the magnetic moments at the Fe sites.

odd under \mathcal{P} . This, together with being odd under \mathcal{T} illustrates that this is a magnetic toroidal order parameter.

To understand how this AFM order gives rise to the term $\xi_-(\mathbf{k})$ in Eq. (1), it is useful to consider a simple tight-binding model for $\text{FeSe}_{1-x}\text{S}_x$. In particular, consider a two-dimensional model that only includes xy orbitals on the iron (Fe) sites. The corresponding tight-

binding Hamiltonian is

$$H_0 = [t_1(\cos k_x + \cos k_y) - \mu]\tau_0\sigma_0 + t_2 \cos \frac{k_x}{2} \cos \frac{k_y}{2} \tau_x\sigma_0 + \alpha_R(\sin k_x \tau_z \sigma_y + \sin k_y \tau_z \sigma_x) \quad (4)$$

where α_R term is a Rashba-like spin-orbit coupling [46]. We add to H_0 the Néel AFM order with moments oriented along the \hat{y} -direction. This is given by $T_x \tau_z \sigma_y$. Treating this as a perturbation to the Hamiltonian H_0 yields

$$\xi_-(\mathbf{k}) = \frac{T_x \alpha_R \sin k_x}{\sqrt{t_2^2 (\cos \frac{k_x}{2} \cos \frac{k_y}{2})^2 + \alpha_R^2 (\sin^2 k_x + \sin^2 k_y)}}. \quad (5)$$

More generally, AFM order with moments along the \hat{y} and \hat{x} directions form the 2D E_u irrep with order parameter (T_x, T_y) .

Lifshitz invariant and PDW state.—The simultaneous breaking of time-reversal symmetry and parity symmetry by the magnetic toroidal order allows the existence of a Lifshitz invariant in the Ginzburg Landau (GL) free energy. Both the magnetic toroidal order $\mathbf{T} = (T_x, T_y)$ and $\mathbf{D} = (D_x, D_y)$ (where $\mathbf{D} = -i\nabla - 2e\mathbf{A}$, the charge of the electron $e < 0$, \mathbf{A} is the vector potential, and we work in units such that $\hbar = c = 1$) transforms as an E_u irrep of D_{4h} . Therefore, these can be coupled leading to the Lifshitz invariant

$$\epsilon \mathbf{T} \cdot [\psi(\mathbf{D}\psi)^* + \psi^*(\mathbf{D}\psi)] \quad (6)$$

This Lifshitz invariant guarantees a PDW state with finite momentum pairing [47, 48], in which the superconducting order parameter develops a spatial variation, $\psi = \psi_0 e^{i\mathbf{q}\cdot\mathbf{r}}$. As discussed in the companion paper [44], the PDW state with finite \mathbf{q} alters the Bogoliubov quasi-particle spectrum:

$$E_{\mathbf{k},\mathbf{q},\pm} = \xi_-(\mathbf{k}) + \frac{\hbar}{2} \mathbf{v}_F \cdot \mathbf{q} \pm \sqrt{[\xi_+(\mathbf{k}) - \mu]^2 + |\psi(\mathbf{k})|^2} \quad (7)$$

where \mathbf{v}_F is the Fermi velocity. As shown in the companion paper, the main consequence of \mathbf{q} is to reduce the size of the BFSs [44]. However, the BFSs are generically not fully removed by a non-zero \mathbf{q} .

Superconducting fluctuations and AFM T_c .—For the Néel AFM order to be the origin of the BFSs, it needs to order above the superconducting T_c . While there is no evidence that indicates this occurs, it is possible that the observed μSR signal [49] onsets due to the formation of AFM order that occurs just above the superconducting T_c . This may occur if there is an enhancement of the T_c of the AFM order by superconducting fluctuations. To illustrate this effect, we consider the following minimal free energy density:

$$f = \frac{\kappa}{2} |\nabla\psi|^2 + \frac{\mu}{2} |\psi|^2 + \frac{\alpha_T}{2} |\mathbf{T}|^2 + \epsilon \mathbf{T} \cdot [\psi(-i\nabla\psi)^* + c.c.] \quad (8)$$

By integrating out the superconducting fluctuations, we obtain the correction to α_T :

$$\begin{aligned}\alpha_T \rightarrow \mu_T &= \alpha_T - \frac{1}{2T} \epsilon^2 \langle |\psi|^2 |\nabla\psi|^2 \rangle \\ &= \alpha_T - 2T \epsilon^2 \left(\frac{1}{\Lambda^3} \int^{\Lambda^3} \frac{d^3k}{(2\pi)^3} \frac{1}{\mu + \kappa \mathbf{k}^2} \right) \\ &\quad \times \left(\frac{1}{\Lambda^3} \int^{\Lambda^3} \frac{d^3k}{(2\pi)^3} \frac{k^2}{\mu + \kappa \mathbf{k}^2} \right)\end{aligned}\quad (9)$$

where Λ is the ultraviolet wavelength cutoff. Near the superconducting transition ($\mu \rightarrow 0$), the fluctuations of the superconducting order parameter, $\langle |\psi|^2 \rangle$ and $\langle |\nabla\psi|^2 \rangle$, reach their maximum values allowing the magnetic toroidal order to appear at $\mu_T = 0$. We note that these materials host strong superconducting fluctuations [50] consistent with such a possibility of a superconductivity-driven AFM order.

Spontaneous PDW order.—While the above explanation offers a mechanism for the proximity of the superconducting and the AFM T_c , Eq. (7) suggests a mechanism for which there is only a single T_c at which superconductivity and AFM appear together with BFSs. In particular, this will occur if a spontaneous PDW order appears at T_c (for which $\psi = \psi_0 e^{i\mathbf{q}\cdot\mathbf{r}}$). For this to occur, the stiffness κ in Eq. (8) needs to be less than zero, $\kappa < 0$. While uncommon, there are two mechanisms that could allow this to occur. The first is in a multiband system, where in addition to the usual positive single-band stiffness, there can be negative contributions to the stiffness that arise from quantum geometry [51–53]. The second is that AFM fluctuations can reduce κ , much like superconducting fluctuations reduced α_T [54].

Discussion.—There is one additional consequence of the existence of the Lifshitz invariant in Eq. (6). If we have a current-carrying state in the superconductor, \mathbf{q} becomes nonzero. Since \mathbf{q} and \mathbf{T} are bilinearly coupled, \mathbf{T} will be nonzero. Therefore, we conclude that supercurrents will induce Néel magnetic order in many Fe-based superconductors that have P4/nmm space group symmetry and two Fe ions per unit cell. We further note that the existence of the finite momentum pairing is crucial for the superconducting diode effect [55–58]. This suggests that superconductivity coexisting with the magnetic toroidal order provides a route towards creating the superconducting diode effect.

Recently, we learned that an alternate scenario for the phenomenology of tetragonal $\text{FeSe}_{1-x}\text{S}_x$ has been investigated within a microscopic model with magnetic interactions by Yifu Cao, Chandan Setty, Laura Fanfarillo, Andreas Kreisel, and P. J. Hirschfeld [59].

Conclusion.—We performed a symmetry-based analysis of BFSs that can arise from TRSB for $\text{FeSe}_{1-x}\text{S}_x$. We argued that the most likely origin of TRSB which gives rise to a nematic BFS in the tetragonal phase is a magnetic toroidal order belonging to the E_u representation.

We are able to replicate the momentum dependence to the BFS shape and the minimum quasi-particle excitation energy observed by laser ARPES. We point to two possible origins of the MT order, either through static Néel AFM order or due to the spontaneous formation of PDW superconductivity. We argue that supercurrents will induce Néel magnetic order in many Fe-based superconductors.

We thank Rafael Fernandes, Peter Hirschfeld, Takasada Shibauchi, and Amalia Coldea for useful conversations. This work was supported by the US Department of Energy, Office of Basic Energy Sciences, Division of Materials Sciences and Engineering under Award DE-SC0021971 and by a UWM Discovery and Innovation Grant.

* These authors contributed equally.

- [1] Y. Kamihara, H. Hiramatsu, M. Hirano, R. Kawamura, H. Yanagi, T. Kamiya, and H. Hosono, Iron-based layered superconductor: LaOFeP , *Journal of the American Chemical Society* **128**, 10012 (2006).
- [2] F.-C. Hsu, J.-Y. Luo, K.-W. Yeh, T.-K. Chen, T.-W. Huang, P. M. Wu, Y.-C. Lee, Y.-L. Huang, Y.-Y. Chu, D.-C. Yan, and M.-K. Wu, Superconductivity in the PbO -type structure $\alpha\text{-FeSe}$, *Proceedings of the National Academy of Sciences* **105**, 14262 (2008).
- [3] T. Shibauchi, T. Hanaguri, and Y. Matsuda, Exotic superconducting states in FeSe -based materials, *Journal of the Physical Society of Japan* **89**, 102002 (2020).
- [4] A. Kreisel, P. J. Hirschfeld, and B. M. Andersen, On the remarkable superconductivity of FeSe and its close cousins, *Symmetry* **12**, 1402 (2020).
- [5] A. I. Coldea, Electronic nematic states tuned by isoelectronic substitution in bulk $\text{FeSe}_{1-x}\text{S}_x$, *Frontiers in Physics* **8**, 528 (2021).
- [6] S. Margadonna, Y. Takabayashi, M. T. McDonald, K. Kasperkiewicz, Y. Mizuguchi, Y. Takano, A. N. Fitch, E. Suard, and K. Prassides, Crystal structure of the new FeSe_{1-x} superconductor, *Chemical Communications* **43**, 5607 (2008).
- [7] J. N. Millican, D. Phelan, E. L. Thomas, J. B. Leão, and E. Carpenter, Pressure-induced effects on the structure of the FeSe superconductor, *Solid State Communications* **149**, 707 (2009).
- [8] T. McQueen, A. Williams, P. Stephens, J. Tao, Y. Zhu, V. Ksenofontov, F. Casper, C. Felser, and R. Cava, Tetragonal-to-orthorhombic structural phase transition at 90 K in the superconductor $\text{Fe}_{1.01}\text{Se}$, *Physical Review Letters* **103**, 057002 (2009).
- [9] Y. Mizuguchi, F. Tomioka, S. Tsuda, T. Yamaguchi, and Y. Takano, Substitution effects on FeSe superconductor, *Journal of the Physical Society of Japan* **78**, 074712 (2009).
- [10] J. Guo, H. Lei, F. Hayashi, and H. Hosono, Superconductivity and phase instability of NH_3 -free Na-intercalated $\text{FeSe}_{1-z}\text{S}_z$, *Nature Communications* **5**, 4756 (2014).
- [11] M. D. Watson, T. K. Kim, A. A. Haghhighrad, S. F.

- Blake, N. Davies, M. Hoesch, T. Wolf, and A. I. Coldea, Suppression of orbital ordering by chemical pressure in $\text{FeSe}_{1-x}\text{S}_x$, *Physical Review B* **92**, 121108 (2015).
- [12] S. Moore, J. Curtis, C. Di Giorgio, E. Lechner, M. Abdel-Hafiez, O. Volkova, A. Vasiliev, D. Chareev, G. Karapetrov, and M. Iavarone, Evolution of the superconducting properties in $\text{FeSe}_{1-x}\text{S}_x$, *Physical Review B* **92**, 235113 (2015).
- [13] S. Hosoi, K. Matsuura, K. Ishida, H. Wang, Y. Mizukami, T. Watashige, S. Kasahara, Y. Matsuda, and T. Shibauchi, Nematic quantum critical point without magnetism in $\text{FeSe}_{1-x}\text{S}_x$ superconductors, *Proceedings of the National Academy of Sciences* **113**, 8139 (2016).
- [14] D. F. Agterberg, P. M. R. Brydon, and C. Timm, Bogoliubov Fermi surfaces in superconductors with broken time-reversal symmetry, *Physical review letters* **118**, 127001 (2017).
- [15] P. M. R. Brydon, D. F. Agterberg, H. Menke, and C. Timm, Bogoliubov Fermi surfaces: General theory, magnetic order, and topology, *Physical Review B* **98**, 224509 (2018).
- [16] Y. Sato, S. Kasahara, T. Taniguchi, X. Xing, Y. Kasahara, Y. Tokiwa, Y. Yamakawa, H. Kontani, T. Shibauchi, and Y. Matsuda, Abrupt change of the superconducting gap structure at the nematic critical point in $\text{FeSe}_{1-x}\text{S}_x$, *Proceedings of the National Academy of Sciences* **115**, 1227 (2018).
- [17] T. Hanaguri, K. Iwaya, Y. Kohsaka, T. Machida, T. Watashige, S. Kasahara, T. Shibauchi, and Y. Matsuda, Two distinct superconducting pairing states divided by the nematic end point in $\text{FeSe}_{1-x}\text{S}_x$, *Science Advances* **4**, eaar6419 (2018).
- [18] Y. Mizukami, M. Haze, O. Tanaka, K. Matsuura, D. Sano, J. Böker, I. Eremin, S. Kasahara, Y. Matsuda, and T. Shibauchi, Thermodynamics of transition to BCS-BEC crossover superconductivity in $\text{FeSe}_{1-x}\text{S}_x$, *arXiv preprint arXiv:2105.00739* (2021).
- [19] K. Matsuura, M. Roppongi, M. Qiu, Q. Sheng, Y. Cai, K. Yamakawa, Z. Guguchia, R. P. Day, K. M. Kojima, A. Damascelli, *et al.*, Two superconducting states with broken time-reversal symmetry in $\text{FeSe}_{1-x}\text{S}_x$, *Proceedings of the National Academy of Sciences* **120**, e2208276120 (2023).
- [20] T. Bzdušek and M. Sgrist, Robust doubly charged nodal lines and nodal surfaces in centrosymmetric systems, *Physical Review B* **96**, 155105 (2017).
- [21] J. M. Link and I. F. Herbut, Bogoliubov-Fermi surfaces in noncentrosymmetric multicomponent superconductors, *Physical Review Letters* **125**, 237004 (2020).
- [22] S. Sumita, T. Nomoto, K. Shiozaki, and Y. Yanase, Classification of topological crystalline superconducting nodes on high-symmetry lines: Point nodes, line nodes, and Bogoliubov Fermi surfaces, *Phys. Rev. B* **99**, 134513 (2019).
- [23] H. Oh and E.-G. Moon, Instability of $j = \frac{3}{2}$ Bogoliubov Fermi surfaces, *Physical Review B* **102**, 020501 (2020).
- [24] S.-T. Tamura, S. Iimura, and S. Hoshino, Electronic multipoles and multiplet pairs induced by Pomeranchuk and Cooper instabilities of Bogoliubov Fermi surfaces, *Physical Review B* **102**, 024505 (2020).
- [25] T. Miki, S.-T. Tamura, S. Iimura, and S. Hoshino, Odd-frequency pairing inherent in a Bogoliubov Fermi liquid, *Physical Review B* **104**, 094518 (2021).
- [26] H. Menke, C. Timm, and P. M. R. Brydon, Bogoliubov Fermi surfaces stabilized by spin-orbit coupling, *Physical Review B* **100**, 224505 (2019).
- [27] C. Timm, A. P. Schnyder, D. F. Agterberg, and P. M. R. Brydon, Inflated nodes and surface states in superconducting half-Heusler compounds, *Physical Review B* **96**, 094526 (2017).
- [28] C. Setty, S. Bhattacharyya, Y. Cao, A. Kreisel, and P. J. Hirschfeld, Topological ultranodal pair states in iron-based superconductors, *Nature Communications* **11**, 523 (2020).
- [29] C. Setty, Y. Cao, A. Kreisel, S. Bhattacharyya, and P. J. Hirschfeld, Bogoliubov Fermi surfaces in spin- $\frac{1}{2}$ systems: Model Hamiltonians and experimental consequences, *Physical Review B* **102**, 064504 (2020).
- [30] T. Nagashima, T. Hashimoto, S. Najafzadeh, S.-i. Ouchi, T. Suzuki, A. Fukushima, S. Kasahara, K. Matsuura, M. Qiu, Y. Mizukami, K. Hashimoto, Y. Matsuda, T. Shibauchi, S. Shin, and K. Okazaki, Discovery of nematic Bogoliubov Fermi surface in an iron-chalcogenide superconductor, *Research Square preprint* <https://doi.org/10.21203/rs.3.rs-2224728/v1> (2022).
- [31] V. M. Dubovik and V. V. Tugushev, Toroid moments in electrostatics and solid-state physics, *Physics Reports* **187**, 145 (1990).
- [32] M. Fiebig, Revival of the magnetoelectric effect, *Journal of Physics D: applied physics* **38**, R123 (2005).
- [33] C. Ederer and N. A. Spaldin, Towards a microscopic theory of toroidal moments in bulk periodic crystals, *Physical Review B* **76**, 214404 (2007).
- [34] N. A. Spaldin, M. Fiebig, and M. Mostovoy, The toroidal moment in condensed-matter physics and its relation to the magnetoelectric effect, *Journal of Physics: Condensed Matter* **20**, 434203 (2008).
- [35] Y. V. Kopayev, Toroidal ordering in crystals, *Physics-Uspekhi* **52**, 1111 (2009).
- [36] S. Hayami, H. Kusunose, and Y. Motome, Toroidal order in metals without local inversion symmetry, *Physical Review B* **90**, 024432 (2014).
- [37] P. Tolédano, M. Ackermann, L. Bohatý, P. Becker, T. Lorenz, N. Leo, and M. Fiebig, Primary ferrotoroidicity in antiferromagnets, *Physical Review B* **92**, 094431 (2015).
- [38] S. Gnewuch and E. E. Rodriguez, The fourth ferroic order: Current status on ferrotoroidic materials, *Journal of Solid State Chemistry* **271**, 175 (2019).
- [39] S. Hayami and H. Kusunose, Microscopic description of electric and magnetic toroidal multipoles in hybrid orbitals, *Journal of the Physical Society of Japan* **87**, 033709 (2018).
- [40] S. Hayami, M. Yatsushiro, Y. Yanagi, and H. Kusunose, Classification of atomic-scale multipoles under crystallographic point groups and application to linear response tensors, *Physical Review B* **98**, 165110 (2018).
- [41] S. Hayami, M. Yatsushiro, and H. Kusunose, Nonlinear spin Hall effect in PT-symmetric collinear magnets, *Physical Review B* **106**, 024405 (2022).
- [42] M. Yatsushiro, R. Oiwa, H. Kusunose, and S. Hayami, Analysis of model-parameter dependences on the second-order nonlinear conductivity in PT-symmetric collinear antiferromagnetic metals with magnetic toroidal moment on zigzag chains, *Physical Review B* **105**, 155157 (2022).
- [43] D. F. Agterberg, D. S. Melchert, and M. K. Kashyap, Emergent loop current order from pair density wave su-

- perconductivity, *Phys. Rev. B* **91**, 054502 (2015).
- [44] A. Amin, H. Wu, T. Shishidou, and D. F. Agterberg, submitted to *Physical Review B* (2023).
- [45] S. Kanasugi and Y. Yanase, Anapole superconductivity from PT symmetric mixed-parity interband pairing, *Communications Physics* **5**, 10.1038/s42005-022-00804-7 (2022).
- [46] D. F. Agterberg, T. Shishidou, J. O'Halloran, P. M. R. Brydon, and M. Weinert, Resilient nodeless d-wave superconductivity in monolayer FeSe, *Physical Review Letters* **119**, 267001 (2017).
- [47] V. P. Mineev and K. V. Samokhin, Helical phases in superconductors, *Zh. Eksp. Teor. Fiz* **105**, 747 (1994).
- [48] M. Smidman, M. B. Salamon, H. Q. Yuan, and D. F. Agterberg, Superconductivity and spin-orbit coupling in non-centrosymmetric materials: a review, *Reports on Progress in Physics* **80**, 036501 (2017).
- [49] K. Ishida, Y. Onishi, M. Tsujii, K. Mukasa, M. Qiu, M. Saito, Y. Sugimura, K. Matsuura, Y. Mizukami, K. Hashimoto, and T. Shibauchi, Pure nematic quantum critical point accompanied by a superconducting dome, *Proceedings of the National Academy of Sciences* **119**, e2110501119 (2022).
- [50] S. Kasahara, T. Yamashita, A. Shi, R. Kobayashi, Y. Shimoyama, T. Watashige, K. Ishida, T. Terashima, T. Wolf, F. Hardy, C. Meingast, H. v. Löhneysen, A. Levchenko, T. Shibauchi, and Y. Matsuda, Giant superconducting fluctuations in the compensated semimetal FeSe at the BCS-BEC crossover, *Nature Communications* **7**, 12843 (2016).
- [51] T. Kitamura, A. Daido, and Y. Yanase, Quantum geometric effect on Fulde-Ferrell-Larkin-Ovchinnikov superconductivity, *Physical Review B* **106**, 184507 (2022).
- [52] G. Jiang and Y. Barlas, Pair density waves from local band geometry, *arXiv preprint arXiv:2211.09846* (2022).
- [53] W. Chen and W. Huang, Pair density wave facilitated by Bloch quantum geometry in nearly flat band multiorbital superconductors, *arXiv preprint arXiv:2208.02285* (2022).
- [54] C. Setty, L. Fanfarillo, and P. J. Hirschfeld, Mechanism for fluctuating pair density wave, *Nature Communications* **14**, 3181 (2023).
- [55] N. F. Yuan and L. Fu, Supercurrent diode effect and finite-momentum superconductors, *Proceedings of the National Academy of Sciences* **119**, e2119548119 (2022).
- [56] J. J. He, Y. Tanaka, and N. Nagaosa, A phenomenological theory of superconductor diodes, *New Journal of Physics* **24**, 053014 (2022).
- [57] A. Daido, Y. Ikeda, and Y. Yanase, Intrinsic superconducting diode effect, *Physical Review Letters* **128**, 037001 (2022).
- [58] B. Pal, A. Chakraborty, P. K. Sivakumar, M. Davydova, A. K. Gopi, A. K. Pandeya, J. A. Krieger, Y. Zhang, M. Date, S. Ju, *et al.*, Josephson diode effect from Cooper pair momentum in a topological semimetal, *Nature Physics* **18**, 1228 (2022).
- [59] Y. Cao, C. Setty, L. Fanfarillo, A. Kreisell, and P. J. Hirschfeld, Microscopic origins of ultranodal states in spin-1/2 systems, *arXiv preprint arXiv:2305.15569* (2023).